Supporting information:

Title: Diverging riverine dissolved C:N:P ratios under global environmental change

[1]Ricky Mwangada Mwanake[*],[1]Elizabeth Gachibu Wangari[1], Daniel Graeber[2], Ralf Kiese[1]

[1]Karlsruhe Institute of Technology, Institute for Meteorology and Climate Research, Atmospheric Environmental Research (IMK-IFU), Kreuzeckbahnstrasse 19, Garmisch-Partenkirchen 82467, Germany

[2]Department of Aquatic Ecosystem Analysis, Helmholtz-Centre for Environmental Research–UFZ

*Corresponding author email: ricky.mwanake2@kit.edu

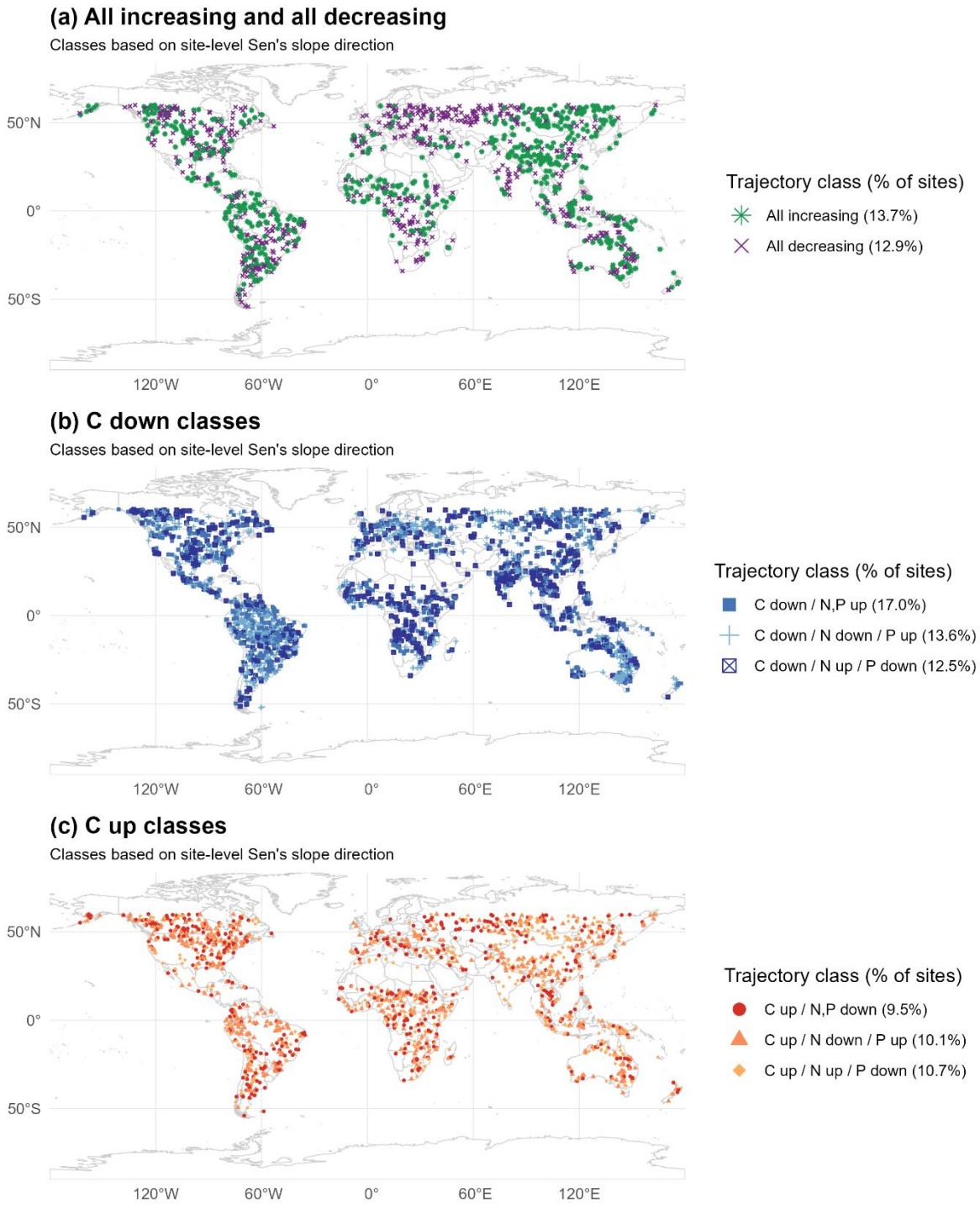

Figure S1: Distribution of trend classes across the 5084 catchments grouped as a) increasing or decreasing trends for DOC, TDN, and TDP, b) decreasing trends of DOC with other combinations for TDP and TDN trends, and c) increasing trends of DOC with other combinations of TDN and TDP trends. The trends were based on median annual rates from Sens's slope estimates after 1000 Monte Carlo simulations to account for model uncertainties in the trend analysis.

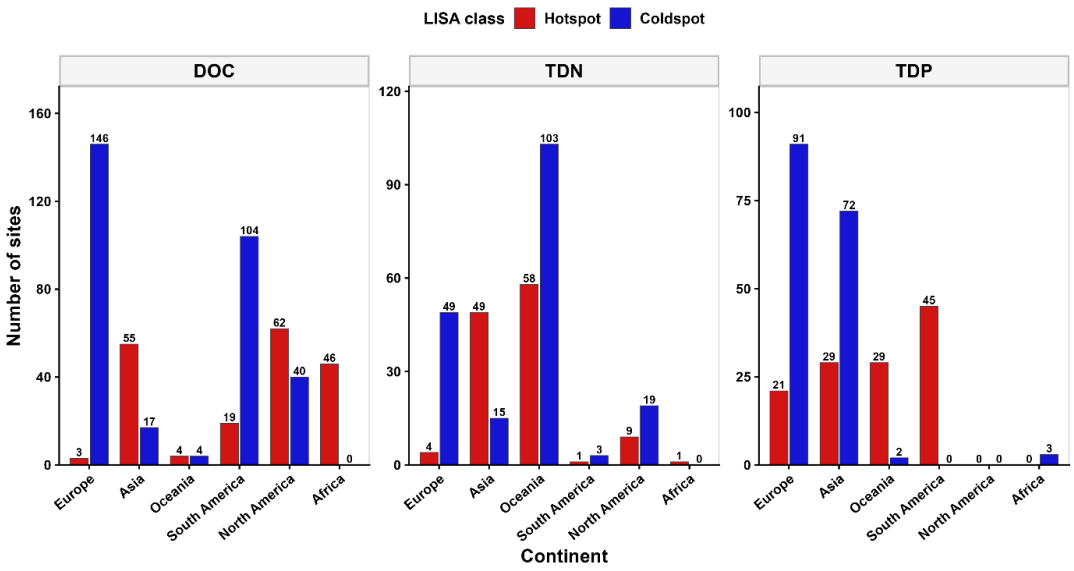

Figure S2: Continental distribution of hotspot (strong increasing trends) and coldspot (strong decreasing trends) sites of DOC, TDN, and TDP 20-year trends. The trends were based on median annual rates from Sens's slope estimates after 1000 Monte Carlo simulations to account for model uncertainties in the trend analysis.

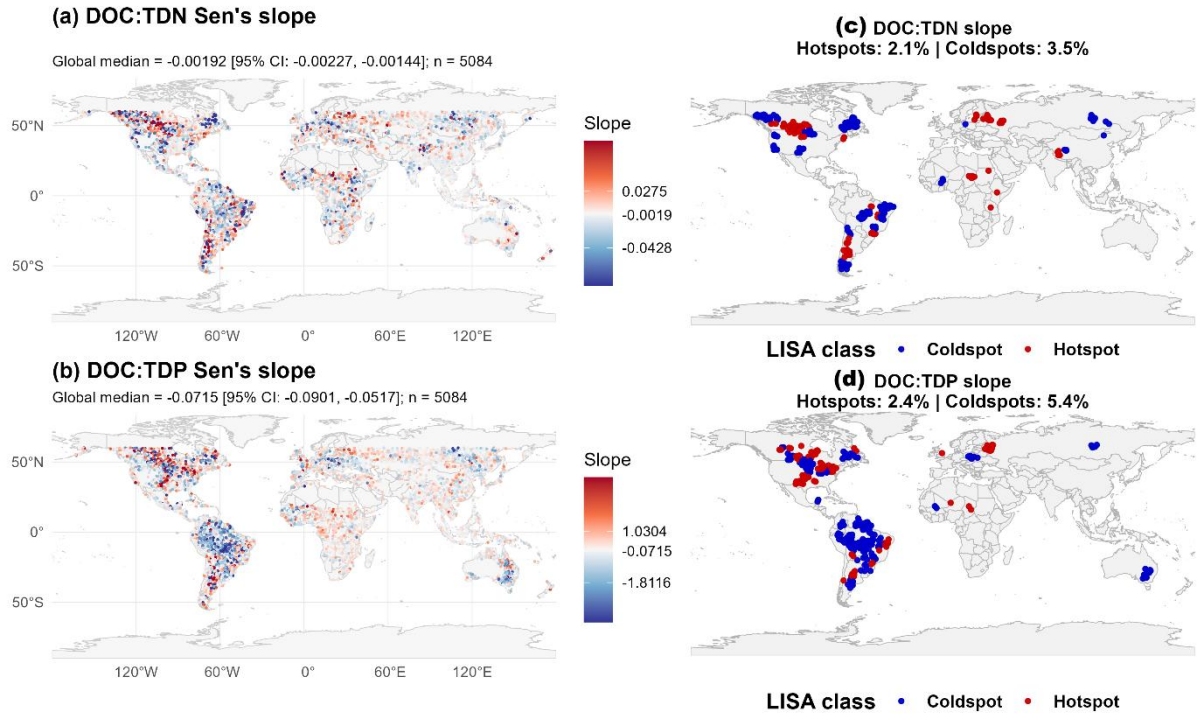

Figure S3. Global distribution of the median (±95% CI) annual rates of change of (a) DOC:TDN and (c) DOC:TDP from 2002 to 2022 (blues = declining trends and reds = increasing trends) at the 5084 catchments. (b, d) shows the global distribution of hotspots (strongly increasing trends) and coldspots (strongly decreasing trends) from these median ratios. Percentages represent the total amount of these sites relative to the 5084 catchments.

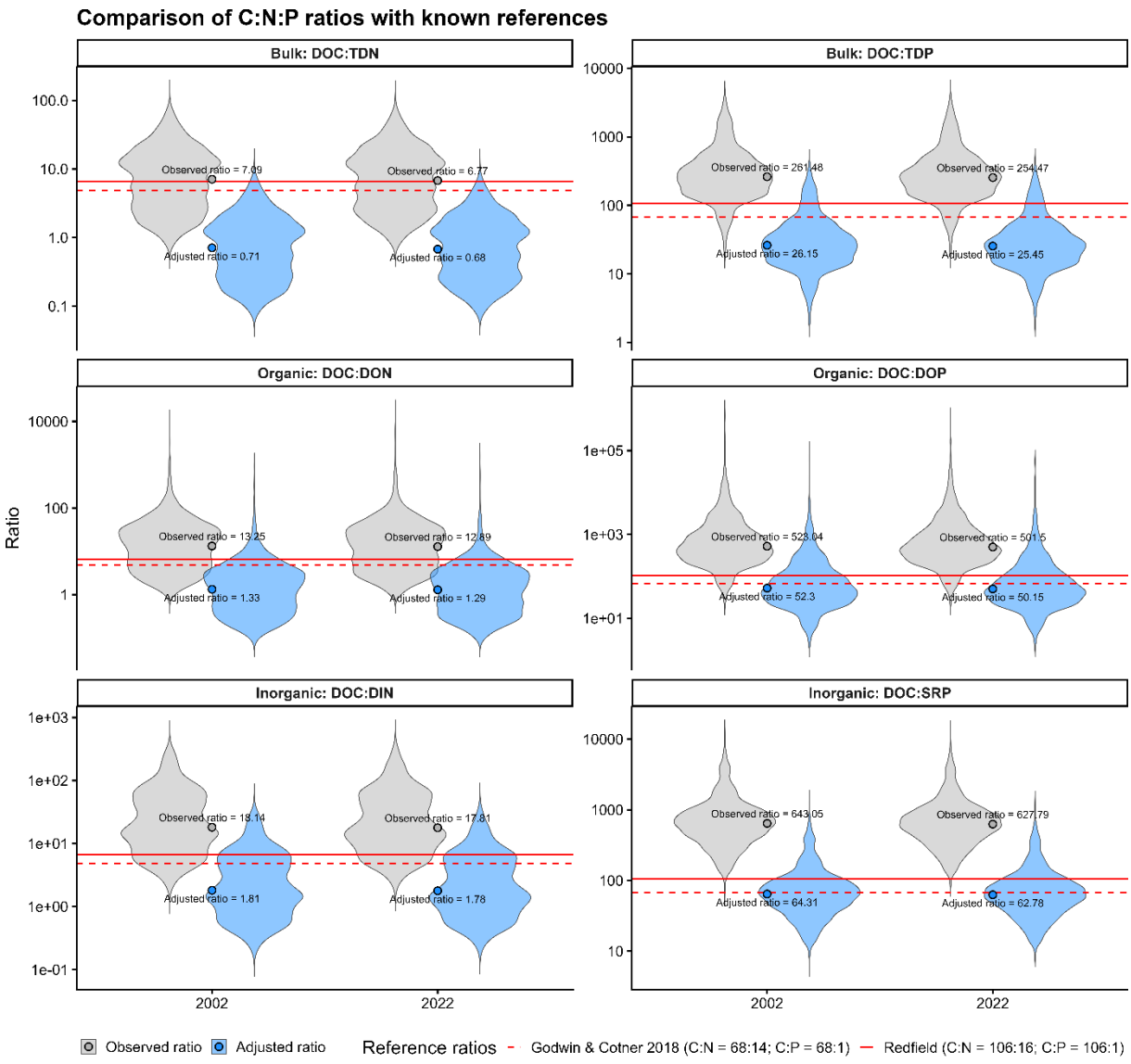

Figure S4. Violin plots showing a comparison of the observed DOC: nutrient molar ratios (in grey) as well as their adjusted ratios (in blue) calculated by assuming that only 10% of the DOC is bioavailable from the 5084 catchments for the years 2002 and 2022. Numbers and text indicate the observed median ratio (assuming 100% DOC bioavailability) and the adjusted median ratio (assuming 10% DOC bioavailability). The red dotted and the red straight lines represent the median ratio of aquatic microbes from Godwin & Cotner, 2018[29], representing the heterotrophic optimum and the Redfield ratio from marine phytoplankton[28] ,representing the autotrophic optimum.

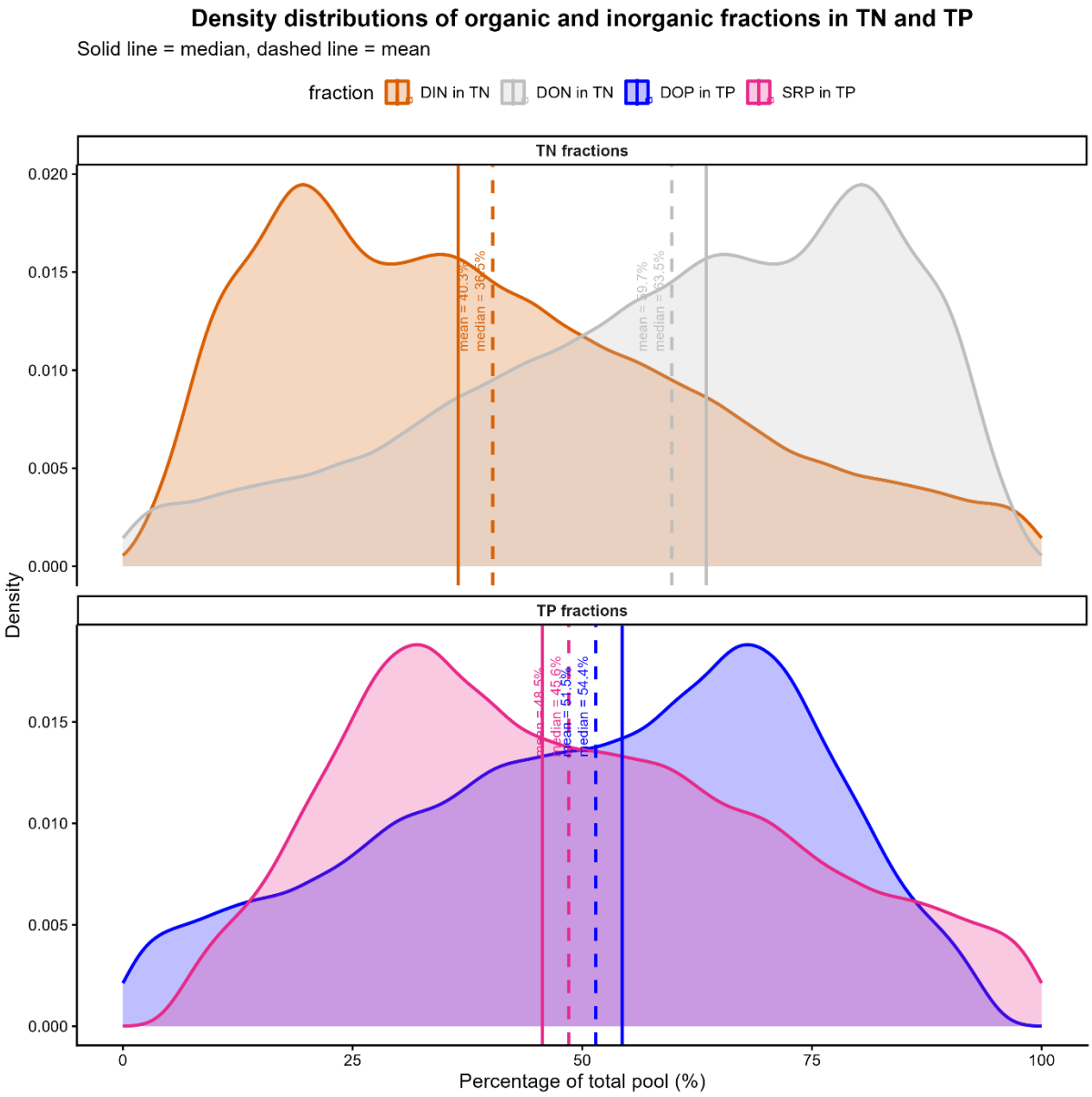

Figure S5. Contributions of organic and inorganic dissolved N and P to their total bulk concentrations. Solid lines indicate the median, while dashed lines indicate the mean across all 5084 catchments for the entire 20-year period.

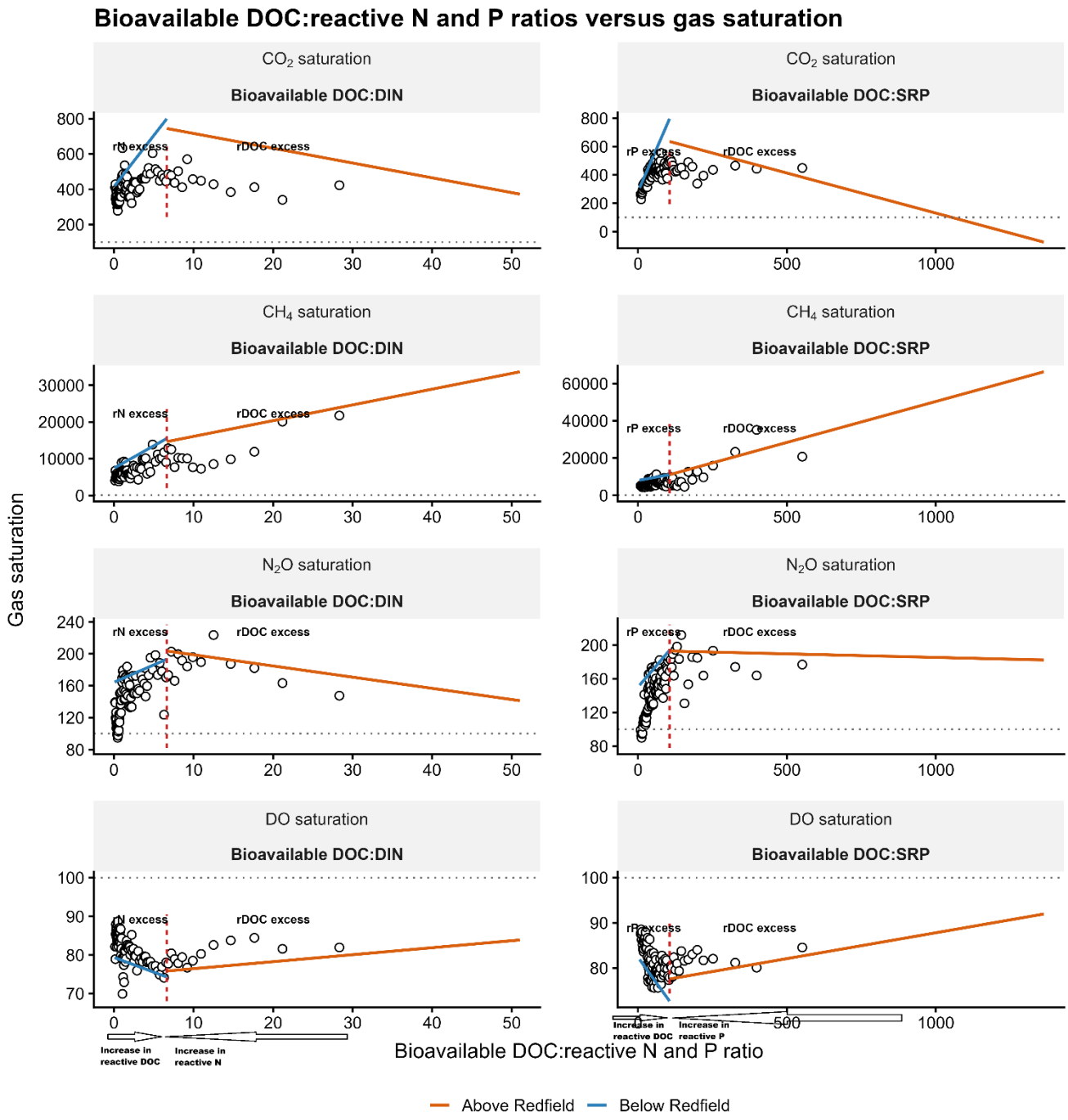

Figure S6. Effects of changing reactive DOC-to-nutrient ratios on GHG and DO saturation. Points indicate binned (100) medians across the 5084 catchments. Dotted vertical lines indicate the Redfield ratio, separating the zones of reactive nutrient excess (left) and reactive DOC excess (right). Solid lines indicate linear trends above and below the Redfield ratios.

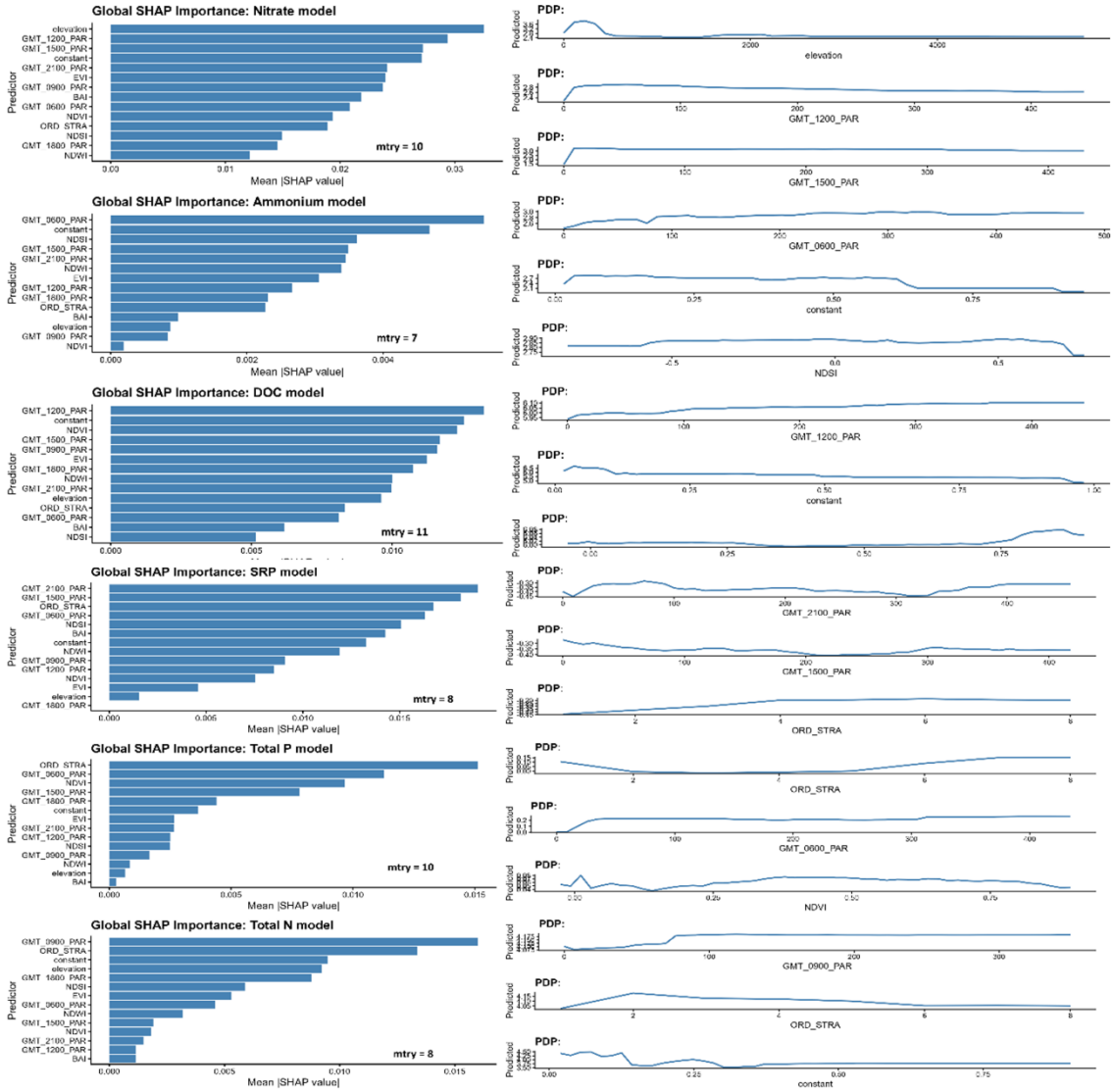

Figure S7: Left Panel displays the relative importance (SHAP analysis) of all 14 predictors from the Random Forest models predicting DOC, TDN, TDP, SRP, NH_4, and NO_3 concentrations, while Right Panel shows partial dependence plots for the three most influential predictors. The most important hyperparameter (mtry= number of predictors in each tree node) calibrated during the model construction is also included. The observed relationships between the top three predictors and response variables mainly aligned well with mechanistic expectations. For example, the topographic diversity constant, a potential proxy for biodiversity, was negatively associated with fluvial TDN and NH_4. This suggests that more biodiverse landscapes, potentially representing more natural landscapes, tend to have lower fluvial nutrient levels than less diverse regions that may be more human-influenced.

The negative relationship between stream order and TDN agrees with established mechanisms; smaller streams often have higher TDN due to stronger connectivity with groundwater and surrounding terrestrial ecosystems compared to larger rivers. Opposite trends were observed for SRP and TDP, with both increasing with stream order, suggesting that sediment accumulation downstream may favor the release of bound P into surface waters.

Some relationships with vegetation indices further supported mechanistic interpretations. For example, the positive association between NDVI and DOC suggests that higher inputs of terrestrial OM support higher DOC concentration.

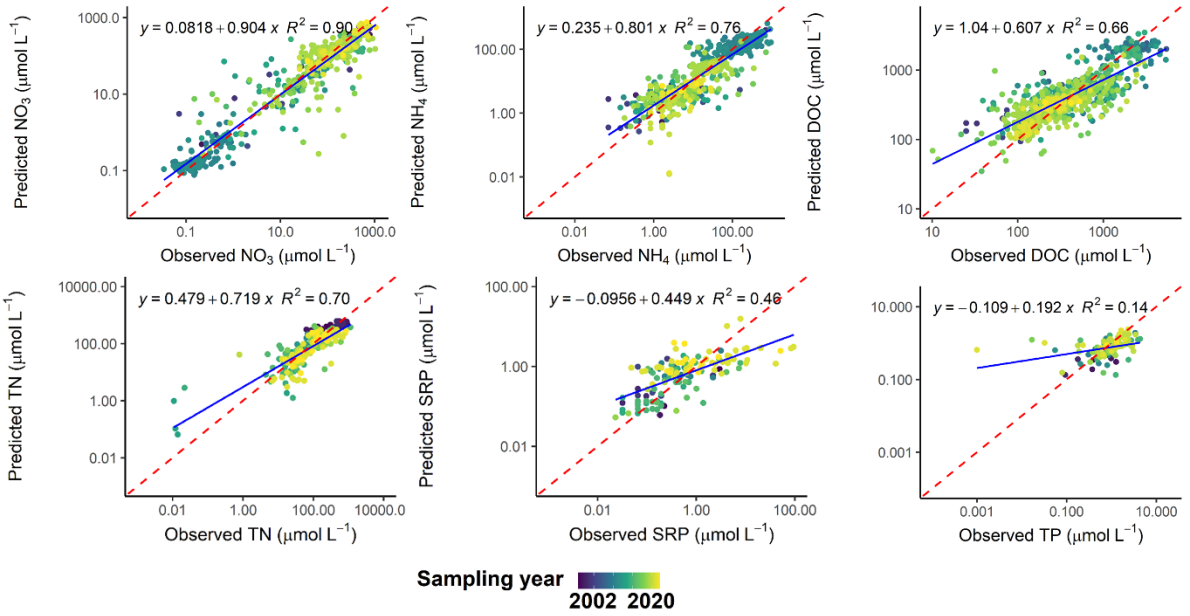

Figure S8: Observed vs predicted plots for DOC, NO_3, NH_4, TDN, SRP, and TDP concentrations derived from 30% of the global dataset excluded from model training. The predictions were done on a daily time step using only remotely sensed parameters. The dotted red line represents the 1:1 line.

Table S1: Modeled annual means of DOC, NO_3, NH_4, TDN, SRP, and TDP concentrations from 5084 globally distributed catchments from 2002 to 2022. The catchments do not include desert or tundra regions. Uncertainties were estimated as the percentage of the mean absolute error from the random forest models relative to the observed empirical means from the measured global datasets. Average Kling-Gupta Efficiency values to assess the temporal skill of the RF models across all the sites with empirical data are also included.

	Predicted annual reach scale values						
Variable	**Number of modeled reaches**	**Temporal duration**	**Range**	**Mean±SE**	**r^2**	**Uncertainty % (MAE/measured mean)**	**KGE value**
NH_4 (µmol L^{-1})	5084	2002 - 2022	0.19 - 334.01	12.44 ± 0.05	0.75	15.6	0.57
NO_3 (µmol L^{-1})	5084	2002 - 2022	0.12 - 624.37	29.3 ± 0.13	0.90	13.4	0.61
DOC (µmol L^{-1})	5084	2002 - 2022	44.62 - 2665.79	483.52 ± 0.98	0.64	6.8	0.44
TDN (µmol L^{-1})	5084	2002 - 2022	0.72 - 525.58	83.36 ± 0.24	0.70	13.5	0.39
SRP (µmol L^{-1})	5084	2003 - 2022	0.06 -5.80	0.88 ± 0.001	0.44	75.7	0.18
TDP (µmol L^{-1})	5084	2002 - 2022	0.18 - 12.26	1.72 ± 0.004	0.53	47.2	0.30